Regional Earth–Atmosphere Energy Balance Estimates Based on Assimilations with a GCM

MICHAEL A. ALEXANDER

Department of Meteorology and Center for Climatic Research, University of Wisconsin, Madison, Wisconsin

SIEGFRIED D. SCHUBERT

Laboratory for Atmospheres, NASA/Goddard Space Flight Center, Greenbelt, Maryland

(Manuscript received 21 April 1989, in final form 10 August 1989)

ABSTRACT

The column budget technique described by Oort and Vonder Haar (1976) is used to assess the physical consistency and accuracy of estimates of the earth–atmosphere energy balance. Regional estimates of the atmospheric budget terms, the net radiation at the top of the atmosphere, and the time tendency and flux divergence of energy are calculated for the Special Observing Periods of the FGGE year. The data are assimilated by the Goddard Laboratory for the Atmospheres (GLA) four-dimensional analysis system. Ocean heat storage is obtained from marine temperature records while the energy flux through the surface and ocean heat flux divergence are computed as residuals.

During winter the midlatitude oceans supply large quantities of energy to the overlying atmosphere which then transports the energy to the continental heat sinks; the energy flows in the opposite direction during summer. The energy exchange between continental and oceanic regions is much stronger in the Northern Hemisphere where land coverage and land–sea differences are greater.

The uncertainties in the energy balance calculations are assessed by examining the errors in the observations, the data assimilation system including the GLA general circulation model, and the energy budget procedures. Sensitivity tests, error analyses and comparison with other studies indicate that the uncertainties in the continental-scale atmospheric energy flux divergence and the surface energy flux are approximately 20 W m^{-2} and 30 W m^{-2}, respectively. We conclude that at present it is not possible to estimate accurately the ocean heat divergence and transport using the column budget technique.

1. Introduction

The storage and transfer of energy in the atmosphere–ocean system play an important role in determining the mean climate and in the evolution of climatic anomalies. Energy budgets have proven to be extremely useful in examining the processes which affect climate by providing a balanced account of the storage, flux divergence, sources and sinks of energy for a given region (Sellers 1965; Palmén and Newton 1969). However, large gaps in the conventional data network (i.e. radiosondes, ship reports etc.), especially over the oceans, high latitudes and Southern Hemisphere, may greatly degrade budget analyses in these regions (Oort 1978). General circulation models (GCMs), in conjunction with data assimilation systems that can accommodate satellite observations, can be used to fill these data gaps and have the potential to provide more accurate estimates of the energy budget components. The high temporal and spatial resolution of datasets generated by model assimilation systems allows for the estimation of the interannual variability of climatic variables on both regional and global scales. The purpose of this study is to assess the accuracy of regional energy balance calculations obtained from model-processed datasets.

With the advent of radiosondes in the 1940s, an aerological data network was established, enabling atmospheric energy budget studies to be conducted. Studies that have examined the zonally averaged atmospheric energy balance include those by Vonder Haar and Oort (1973), Newell et al. (1974), and Oort and Vonder Haar (1976). Limited-area energy statistics are difficult to obtain from aerological networks due to the highly variable nature of some budget components and mass imbalances associated with errors in the wind field, though estimates have been made by Hastenrath (1966) for the Caribbean, Gruber (1970) for the Florida peninsula, and Alestalo (1981) for Europe. Recent studies, such as Sävijarvi (1982), Sävijarvi (1983), Lorenc and Swinbank (1984), Burridge

Corresponding author address: Mr. Michael A. Alexander, Center for Climatic Research, Institute for Environmental Studies, University of Wisconsin-Madison, 1225 W. Dayton Street, Madison, WI 53706.

(1985), Boer (1986) and Holopainen and Fortelius (1986), have utilized data assimilation systems to obtain regional energy balance estimates.

An assimilation system periodically inserts data into a GCM integration, thereby constraining the model to remain in a state close to that of the observed atmosphere. The benefits of using data obtained from assimilation schemes include: (i) an automated and objective method of obtaining complete datasets; (ii) a means of estimating terms which are difficult to measure, e.g., vertical velocity and; (iii) suppression of inconsistencies in the data via the dynamic and conservation requirements which operate during the model forecast period.

However, model-assimilated observations are still prone to both random and systematic errors in the data. In addition, the assimilation procedure can introduce errors into atmospheric diagnostics due to imbalances created during data insertion, interpolation of the data to fit the model grid, and deficiencies in the GCM. The use of multiple observing systems with different sampling frequencies, densities, and biases causes added uncertainty in energy budget analyses.

The high quality and global coverage of the data collected during the First GARP (Global Atmospheric Research Program) Global Experiment (FGGE) allows for detailed study of large-scale atmospheric processes in regions which previously had poor data coverage. In this study, data from the two FGGE Special Observing Periods (SOPs) are used in conjunction with the Goddard Laboratory for Atmospheres (GLA) assimilation system to calculate the atmospheric energy budget components, the storage and flux divergence of energy, and the net radiative flux at the top of the atmosphere. The flux of energy across the surface is derived as a residual from the atmospheric budget analysis.

In contrast to calculations with atmospheric data, the direct measurement of the ocean energy budget components is extremely difficult due to the limited number of velocity measurements. In the present study, the ocean heat transport is obtained from the column budget method (Vonder Haar and Oort 1973; Oort and Vonder Haar 1976; and Carissimo et al. 1985), which utilizes the conservation of energy in the earth–atmosphere system. By computing the atmospheric energy balance, the net flux of energy from the atmosphere to the ocean can be estimated. This energy is either stored (mainly as heat) or redistributed via the divergence of heat by ocean currents. With ocean heat storage estimated from hydrographic data, the ocean heat flux divergence is calculated as a residual. The heat transport can then be computed by integrating the heat flux divergence over the boundary of the region.

Hastenrath (1980) indicated that error estimates, while essential to energy budget studies, are unsatisfactory at present. We will attempt to assess the uncertainty in the energy balance calculations due to errors in the data and data assimilation procedures, the GLA GCM, and in the energy budget procedures. Six separate approaches are used to investigate the accuracy of the energy balance components:

1) Energy flux divergence estimates from this and other studies are compared.

2) Random and systematic errors in the atmospheric variables are inserted into the budget calculations to determine their impact on the storage and flux divergence of energy.

3) Energy flux divergence estimates calculated from the data analyzed on the model grid are compared to the divergence estimates from the 6-hour forecast, which verifies for the same time.

4) Estimates of the shortwave radiation absorbed by the earth–atmosphere system, outgoing longwave radiation, and net radiation at the top of the atmosphere from the GLA GCM are compared with estimates of these quantities derived from satellite data.

5) Budget results obtained by using either pressure or sigma (normalized pressure) as the vertical coordinate system in the atmosphere are compared.

6) The combined surface sensible and latent heat flux obtained as a residual from the column budget method is compared to estimates from the GLA GCM surface flux parameterizations.

2. The budget equations

The column budget method is based on the conservation of total energy in the earth–atmosphere system. Following Oort and Vonder Haar (1976), this can be expressed as

$$S_A + S_O = F_T - \mathrm{div}F_A - \mathrm{div}F_O \qquad (2.1)$$

for the entire budget column (shown schematically in Fig. 1), or for the atmosphere and ocean separately as

$$S_A = F_T - F_S - \mathrm{div}F_A \qquad (2.2)$$

$$S_O = F_S - \mathrm{div}F_O; \qquad (2.3)$$

F_T and F_S are the net flux of energy at the top of the atmosphere and at the earth's surface, respectively. The storage and flux divergence of energy in the atmosphere and ocean are

$$S_A = \frac{\partial}{\partial t}\int_{P_T}^{P_S}(K + c_pT + Lq)\frac{dp}{g} \qquad (2.4)$$

$$\mathrm{div}F_A = \int_{P_T}^{P_S}\nabla\cdot(K + c_pT + gz + Lq)\mathbf{V}\frac{dp}{g} \qquad (2.5)$$

$$S_O = \frac{\partial}{\partial t}\int_d^0\left(K + c_0T + \frac{P}{\rho} + gz\right)\rho dz \qquad (2.6)$$

$$\mathrm{div}F_O = \int_d^0\nabla\cdot\left(K + c_0T + \frac{P}{\rho} + gz\right)\mathbf{V}\rho dz \qquad (2.7)$$

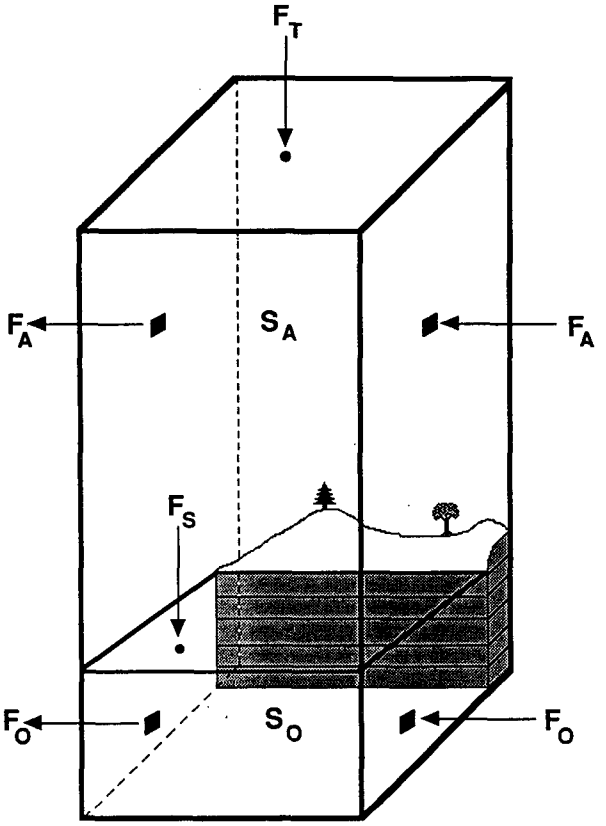

FIG. 1. Schematic of the earth–atmosphere energy balance adapted from Oort and Vonder Haar (1976); F indicates an energy flux and S energy storage; the subscripts A and O represent the atmosphere and ocean, respectively, subscript T denotes the top of the atmosphere and S the earth's surface.

where K is the kinetic energy, c_p the specific heat of air at constant pressure, T the temperature, L the latent heat of vaporization, q the specific humidity, z the height, V the horizontal wind vector, P the pressure, ρ the density, and c_0 the specific heat of sea water. The lower boundary, d, is the depth at which there are assumed to be no vertical fluxes of energy. As the ocean is nearly hydrostatic, incompressible, and has relatively little kinetic energy, only the sensible heat (c_0T) is kept in Eqs. (2.6) and (2.7) (Bryan 1962).

We have neglected some of the components of the earth–atmosphere energy balance in the equations above. The energy stored by land and ice have not been included as they appear to be small when compared to the oceanic storage (Oort and Vonder Haar 1976). The energy transported by ice and by horizontal turbulence (i.e., subgrid scale fluxes) is also neglected, as are the direct effects of electrical, geothermal, and biological processes.

Defining downward fluxes to be positive, the net radiative flux at the top of the atmosphere is

$$F_T = SW_A + SW_S - LW_T \qquad (2.8)$$

where SW_A is the shortwave radiation absorbed in the air column, SW_S the shortwave radiation absorbed at the surface, and LW_T the outgoing longwave radiation flux at the top of the atmosphere. This formulation is used to accommodate the GLA model which computes the absorption of shortwave radiation and the flux of longwave radiation. The net flux of energy at the surface, F_S, includes the net radiative flux, R, minus the upward fluxes of sensible, SH, and latent heat, LH, written as

$$F_S = R - (SH + LH) \qquad (2.9)$$

where the relatively small amount of kinetic energy transferred between the atmosphere and ocean is neglected.

The time and spatial derivatives in the budget equations are represented by second-order finite difference approximations. As the ocean quantities are given by monthly averages, S_O values are obtained from the difference in heat content between the month following and preceding the FGGE SOPs. The atmospheric budget components are computed on 12 pressure levels by first interpolating diagnostics from the model's 9 sigma levels. Vertical integration is performed by a cubic spline method. The limits of integration are between 50 mb and the area average surface pressure in the atmosphere, and from the surface to a depth of 1000 m in the ocean. Inconsistencies in the energy balance calculations arising from differences between the finite differencing used to obtain the budget components and those employed by the GLA GCM are addressed in section 4c.

3. Data processing

a. The model and data assimilation system

The GLA GCM (see Kalnay et al. 1983) is a 9-layer, sigma (σ) coordinate, primitive equation model with a horizontal resolution of 4° latitude by 5° longitude. The model utilizes a fourth-order differencing scheme on an unstaggered grid that conserves energy, and, in combination with a 16-point Shapiro filter (1970), approximately conserves enstrophy and mass. A high latitude Fourier filter is applied poleward of 60° to avoid computational instability. Large-scale cloudiness occurs in the GCM when the relative humidity would otherwise exceed 100%. The sub-grid scale convective parameterization generates cumulus clouds where the air rises moist adiabatically as determined by the moist static stability of successive layers. Both the flux of longwave and the absorption of shortwave radiation are computed explicitly and depend on the humidity and the amount and type of clouds. The surface sensible and latent heat fluxes are derived from bulk aerodynamic formulae based on the local wind speed, stability, and surface drag.

The GCM is part of a four-dimensional assimilation system (Baker 1983) where data are periodically inserted into an extended model integration. Observations are checked for errors and then incorporated into the model integration at 6-hour intervals (0000, 0600, 1200, and 1800 UTC), with the data grouped in 6-hour periods centered on the data insertion time. The observations are included by successively modifying a first-guess field, provided by the 6-hour forecast of the GLA GCM, using a Cressman-type objective analysis scheme (1959). The GLA assimilation system does not include an initialization procedure to remove mass imbalances; however, the damping properties of the time and space differencing schemes in the GLA GCM suppress these imbalances. The atmospheric diagnostics used in the budget calculations are, therefore, extracted from the 6-hour forecast (the first-guess field), prior to the next data insertion.

b. Data sources

During FGGE a heterogeneous collection of observing systems (listed in Table 2 of Baker et al. 1987) provided measurements of atmospheric temperature, pressure, wind and humidity. During the two FGGE special observation periods (SOP I, 5 January through 5 March 1979, and SOP II, 1 May through 31 July 1979) additional data were collected, primarily in tropical regions. The results of this study are based on data collected during the SOPs which were then processed in a delayed mode by an assimilation system to form the GLA FGGE level IIIb dataset.

The oceanic temperatures used to calculate ocean heat storage (S_O) are based on climatological data from the National Oceanographic Data Center (NODC) compiled by Levitus (1982). Due to a lack of synoptic oceanographic data for individual years, monthly mean temperature fields based on all observations regardless of the year are used to compute S_O. The dataset consists of approximately 500 000 casts from hydrographic stations obtained prior to the first quarter of 1977 and 785 000 bathythermographs collected through the first quarter of 1978. To obtain gridded fields, observations were averaged within a 1° by 1° square at each of the 19 NODC standard levels located between the surface and 1000 m. An objective analysis consisting of a Cressman-type interpolation scheme and 5-point smoother provided temperature values at grid points with no data and reduced the effects of spurious observations.

The atmospheric budget components are calculated from 6-hourly data of the FGGE year, while the ocean heat storage is computed from monthly averaged data from a historical record spanning 70 years. Due to the different time scales of the two data sources, our results can not provide entirely consistent quantitative estimates of the earth–atmosphere energy balance. However, the budget analysis is useful for investigating the physical consistency and error characteristics of the energy balance components.

c. Mass balance correction

A major obstacle in computing the atmospheric energy budget is that wind data are not generally mass conserving (Gruber 1970; Alestalo 1981; Sävijarvi 1982). Diagnostics based on analyses from model assimilation systems also suffer from this problem, although it is somewhat reduced (Burridge 1985). In the present study, a correction is applied to the assimilated data which ensures that the regional mean mass divergence is equal to zero. Following Alestalo (1981), the mass balance correction term may be expressed as

$$\left\langle \widehat{(\nabla \cdot \bar{\mathbf{V}})} \int_{50}^{P_S} \bar{e} \frac{dp}{g} \right\rangle, \tag{2.10}$$

where e is any of the four energy quantities, $\langle\ \rangle$ the spatial average and $\widehat{\ }$ the vertical average. The correction is applied by subtracting (2.10) from the original energy flux divergence estimate at each level, effectively shifting the divergence profile while maintaining its shape. Other corrections are possible; for example, the mass adjustment may be taken to have a linear distribution with pressure (O'Brien 1970). Alestalo also examined the latter method but found it gave results similar to the constant adjustment correction described above.

4. Results and discussion

a. Energy budget analysis

Seven budget regions (Fig. 2) were selected to examine the seasonal extremes and continent–ocean differences in the climate system and to compare the results obtained here with other studies. The time-mean energy balance during SOP I and SOP II, presented in Figs. 3 and 4 respectively, indicate that the budget terms undergo strong seasonal variations in all seven regions. Energy is lost to space in winter (SOP I in the Northern Hemisphere (NH), SOP II in the Southern Hemisphere (SH)) and gained in summer via F_T, except for region 6 that gains energy in both seasons as it is partially located in the tropics. The net radiation values are approximately 30 W m^{-2} lower in continental than in oceanic regions during summer but are about the same in winter; a result which has also been documented by Bretherton et al. (1982) and Jacobowitz et al. (1984b). The lower values of F_T over the continents can be attributed to the higher albedo of land which causes more solar radiation to be reflected to space. This effect is substantially reduced in winter due to the reduction in insolation and the relatively large fraction of ocean covered by low level, highly reflective clouds.

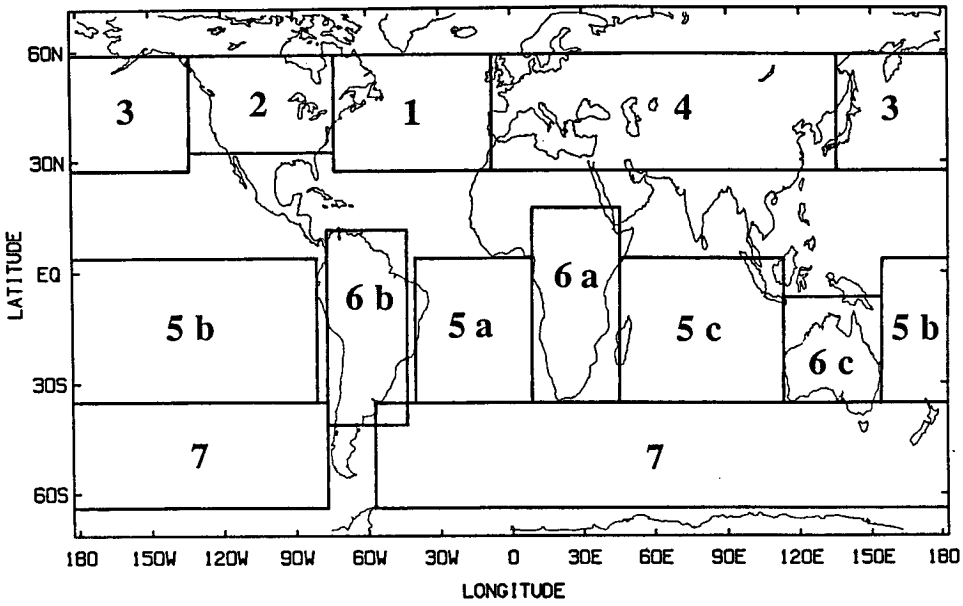

FIG. 2. Regions used in the energy budget analysis.

The time rate of change of energy in the atmosphere (S_A) is generally less than 15 W m^{-2} and therefore plays a small role in the energy balance. During SOP I (late winter in the Northern Hemisphere) S_A is small and positive as the atmospheric energy content remains relatively constant or increases slightly. During SOP II, the atmosphere gains (loses) energy in the Northern Hemisphere (Southern Hemisphere) mainly due to an increase (decrease) in sensible heat. The S_A values obtained here are in general agreement with those of Oort and Vonder Haar (1976), who computed budget statistics from monthly mean data averaged over 10° latitude bands.

The horizontal energy flux divergence is an important component of the atmospheric energy balance, having the same order of magnitude as the net radiation. The Northern Hemisphere values obtained for divF_A indicate energy export (div$F_A > 0$) from oceanic to continental regions during winter, in response to the differential heating characteristics of land and water. The NH oceans store large amounts of energy during summer, as indicated by the large positive values of S_O (Fig. 4) and release this energy to the atmosphere via fluxes of sensible and latent heat during winter (Fig. 3). Some of this energy received by the atmosphere is exported to continents which are heat sinks in winter, while the remainder is lost to space or transported poleward. Due to the small heat capacity and shallow layer of heating of rock and soil, continents gain heat more rapidly and reach a higher temperature than the oceans during spring and summer. This energy is imparted to the overlying air which transports it to oceanic regions. The land areas in the Southern Hemisphere (region 6a–c) also exhibit this climatic regime but the smaller land mass between 20°S–70°S limits its magnitude.

Energy balance requirements over the continents are such that the flux of energy through the surface equals the energy stored by land (S_L). Gabites (see Oort and Vonder Haar 1976) estimated monthly S_L values to be less than 5 W m^{-2}, requiring similarly small values for F_S. Our estimates of F_S over land, though generally less than half the ocean–air fluxes in the same latitude belt, are likely to be excessive. Estimates of F_S, derived as residuals from Eq. (2.2), are degraded by errors in the other atmospheric budget components and by the inclusion of ocean sections in the "continental" regions (see Fig. 2).

The strong seasonality in F_S leads to an increase in the ocean heat content during summer ($S_O > 0$) and heat loss in winter ($S_O < 0$). The seasonal variation is not so clearly evident in divF_O; whereas heat is imported into the North Atlantic during SOP I and exported during SOP II, the North Pacific and the Southern Hemisphere ocean (region 5) export heat throughout the year. Convergence of F_O supplies heat to the Antarctic Ocean during the Southern Hemisphere winter, but a surprisingly large amount of energy, 62 W m^{-2}, is removed by divF_O in summer. The energy export may result from strong northward heat transport at all latitudes in the Atlantic in response to the large energy sink in the North Atlantic and Arctic Ocean (Hastenrath 1982; Hsiung 1985). The residually derived values of divF_O may be unrealistic due to the dissimilar nature of the atmospheric and oceanic datasets, the paucity of data in oceanic regions, and the large uncertainty in ocean heat storage estimates [discussed in section 4c(1)].

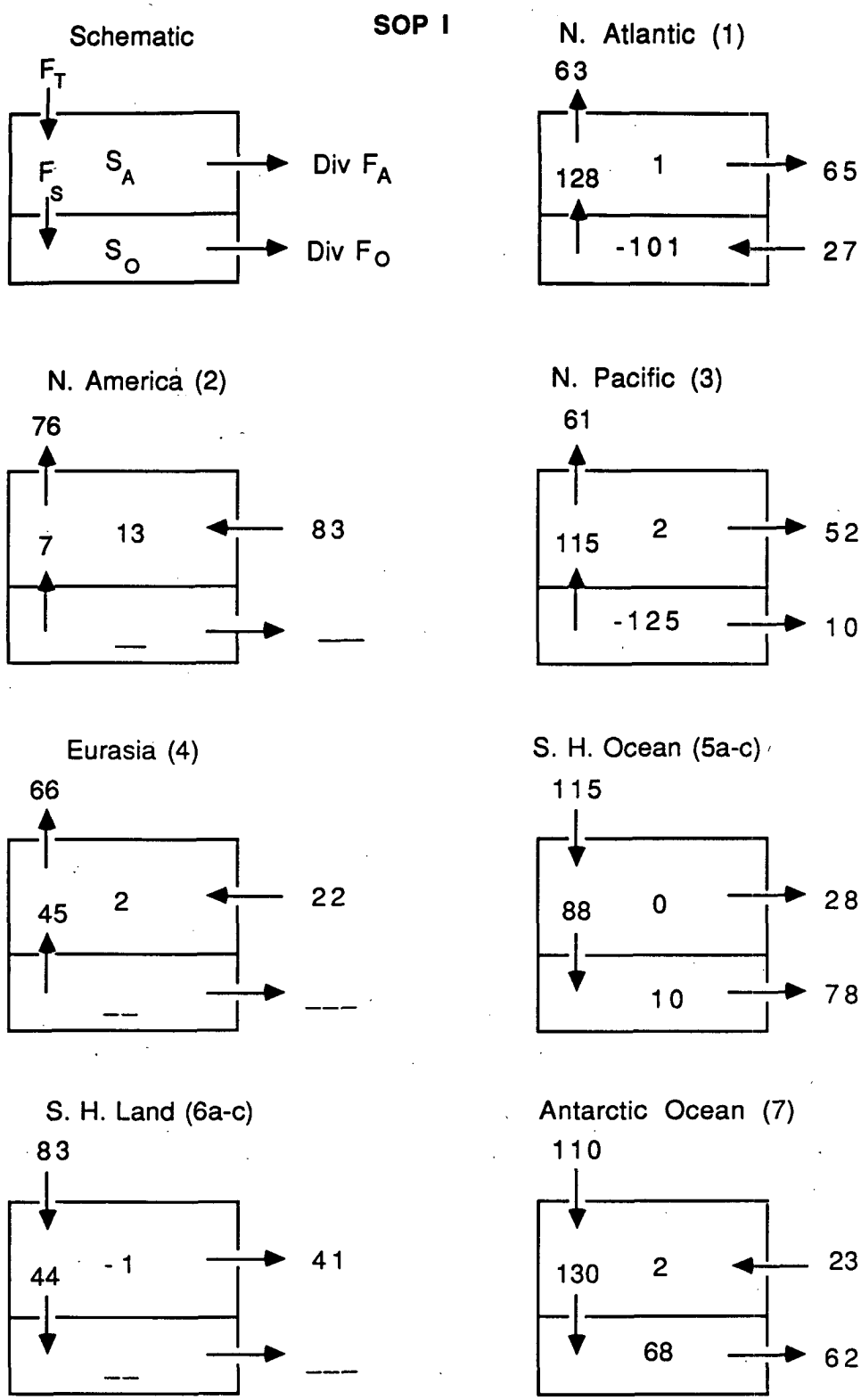

FIG. 3. The atmospheric energy balance terms are depicted in the upper left corner. The energy balance components in W m^{-2} during SOP I are shown for the seven budget regions. The region numbers are in parentheses. The arrowheads show the flow of energy and the dashes indicate that the storage and flux divergence of energy are neglected in the cryosphere.

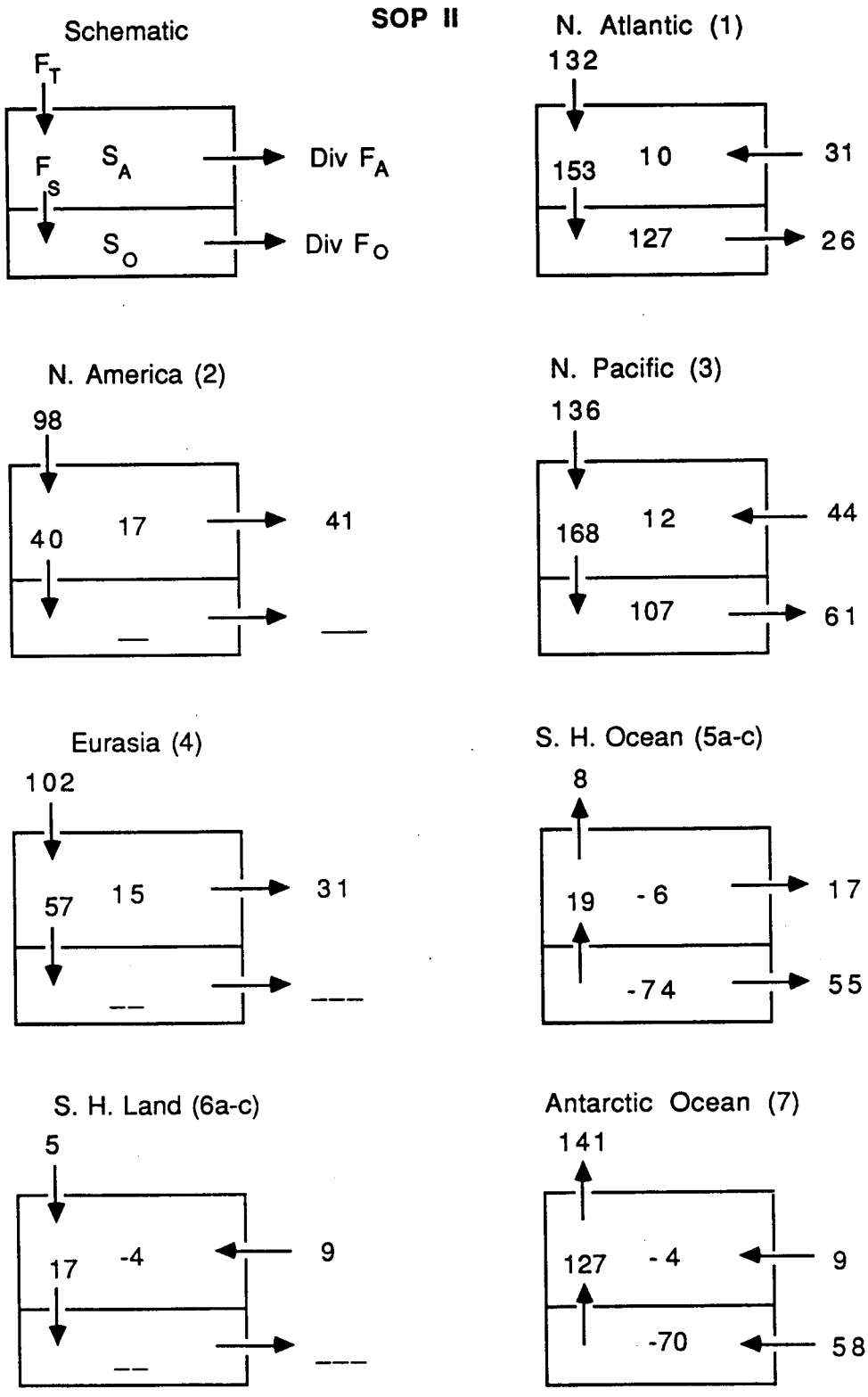

FIG. 4. Same as Fig. 4 except for SOP II.

b. Comparison of atmospheric flux divergence estimates

One method of assessing the accuracy of energy budget estimates is to compare statistics from independent analyses. Lorenc and Swinbank (1984) calculated the atmospheric energy flux divergence from the British Meteorological Office (Met Office) FGGE IIIa analysis described by Lyne et al. (1982) and from the European Centre for Medium Range Weather Forecasts (ECMWF) IIIb analysis (Bengtsson et al. 1982). The characteristics of the two analysis systems have been described and compared by Hollingsworth (1985a) for synoptic forecasts and by Lorenc and Swinbank (1984) with respect to generating general circulation statistics. The budget calculations from the Met Office and ECMWF analysis systems were performed using pressure-level diagnostics. The results from our study using the GLA IIIb pressure analysis are presented along with Lorenc and Swinbank's in Table 1 for July 1979, for the North Atlantic, North America, North Pacific and Eurasian sectors.

The vertically integrated mass divergence in all three analyses (not shown) indicate erroneous long-term mean surface pressure changes; the regional bias in the GLA analyses are on the order of 5 mb d^{-1}. Burridge (1985) estimated that even a 1 mb d^{-1} bias in the surface pressure would result in the adjustment of $\mathrm{div}F_A$ by 40 W m^{-2}, demonstrating the necessity of mass balance corrections. The corrections used to obtain the flux divergence estimates of sensible and geopotential energies in Table 1 are of the same order as the uncorrected values, while insignificant for latent energy.

TABLE 1. The vertically integrated atmospheric energy flux divergence in W m^{-2} for regions 1–4 during July 1979. The results obtained using the GLA assimilation system are presented along with the British Met Office and ECMWF values from Table 2 in Lorenc and Swinbank (1984).

	Energy flux divergence			
	Sensible	Geopotential	Latent	Total
North Atlantic				
Met Office	66	−109	14	−30
ECMWF	41	−80	14	−26
GLA	35	−68	10	−22
North America				
Met Office	−11	40	7	37
ECMWF	−20	40	4	25
GLA	57	−31	10	45
North Pacific				
Met Office	−30	3	−19	−46
ECMWF	−22	−9	−25	−54
GLA	−83	75	20	−41
Eurasia				
Met Office	40	−4	−7	29
ECMWF	42	−10	−12	21
GLA	76	−52	−33	33

After the mass balance correction has been applied, there is relatively good agreement (<30 W m^{-2}) among the three estimates of the flux divergence of c_pT, gz, Lq over the Atlantic. However, large differences occur among the three estimates of sensible and geopotential energy flux divergence in the other three regions. For example, over North America the GLA values indicate sensible heat flux divergence and geopotential energy convergence, which are opposite to the results from the Met Office and ECMWF analyses.

The budget analyses show that the sensible and geopotential energy divergences roughly compensate each other, having the same magnitude but opposite sign. This balance can be attributed to a thermally direct circulation (White and Saltzman 1956; Alestalo 1981); a rising parcel cools adiabatically, decreasing its internal energy while gaining potential energy, whereas the opposite occurs during subsidence. When the sensible and geopotential energies are considered together, the differences between the analyses are substantially reduced, causing the total energy flux divergence estimates to differ by less than 20 W m^{-2}. Energy conservation requirements constrain the total energy divergence while allowing the individual components more degrees of freedom.

The GLA estimates of $\mathrm{div}F_A$ in regions 1–4 differ from the Met Office and the ECMWF estimates by an average of 6 and 12 W m^{-2}, respectively. It is somewhat surprising that the greatest discrepancies in $\mathrm{div}F_A$ occurred between the analyses over North America, which has a dense, homogeneous radiosonde network. Holopainen and Fortelius (1986) examined the diabatic heating, excluding latent heat release (which is approximately equal to the flux divergence of $K + c_pT + gz$ for data averaged over a month or longer) for the same four regions during February 1979 using the GLA and ECMWF analyses. They found the analyses differed by approximately 5 W m^{-2}, except for North America, where the disparity between the analyses was 21 W m^{-2}. They attributed this discrepancy to the area of intense diabatic heating along the east coast of the United States, where small variations in the analysis scheme, model parameterizations, and the location of the budget box can substantially affect regional energy diagnostics.

c. Error analysis

In general, it is difficult to separate the numerous sources of uncertainty in the budget calculations. Deficiencies in (i) the data and data assimilation procedure, (ii) the GCM, and (iii) the budget method itself all contribute to inaccuracy in the budget results. Several experiments are performed which address the potential impact of these three sources of uncertainty on the energy balance estimates. The effect of data errors on the budget results is obtained by assuming that the

6-hour forecast is truth and then superimposing realistic errors on the forecast fields. Model deficiencies are examined by assuming the analyses (the beginning of the data assimilation cycle) are truth and then comparing the budgets derived from the analyses with those obtained from forecasts verifying for the same time. In addition, the GLA model estimates of shortwave, longwave and net radiation are compared with concurrent satellite measurements. Potential errors introduced by numerical approximations in the budget method are examined by comparing the energy budget terms in pressure coordinates with those computed in sigma coordinates using the model's finite differencing scheme.

1) DATA AND DATA ASSIMILATION ERRORS

During the FGGE year several observing systems were employed to measure the atmosphere, each having different error characteristics and sampling distributions. Major sources of error include cloud track wind estimates from geostationary satellites (Kållberg et al. 1982) and temperature profiles obtained from microwave radiometers aboard the Tiros-N polar orbiting satellites (Phillips et al. 1979; Schlatter 1981). The Japanese Meteorological Agency (1981) and Halem et al. (1982) investigated the accuracy of the FGGE data and assimilation systems by comparing analyses from different observing systems. They confirmed the errors in the microwave retrievals and cloud tracked winds, and, in addition, determined that variable data density (e.g., large continent–ocean contrasts) and the lag time between observations and their insertion into the model degraded the analyses. Sources of error in the model assimilation cycle include the interpolation of data from pressure to sigma coordinates, the excitation of high frequency gravity waves, the difficulty of including moisture data, and the analyses of mass and motion fields in the tropics.

Both random and systematic errors in temperature, wind, geopotential height, and humidity measurements will directly affect the estimates of S_A and $\mathrm{div}F_A$. In addition, errors in these variables propagate through the budget calculations, degrading the F_S and $\mathrm{div}F_O$ results. The sensitivity of the energy budget results to random errors is examined using a root mean square (rms) error analysis. The analysis is performed by generating "random errors" and then adding these errors to the atmospheric variables each time the variables are extracted from the model's 6-hour forecast. The random errors are obtained by prescribing errors in the variables as a function of height (Table 2), which are then multiplied by a number generated from a pseudo-normal function (a normal distribution with a mean of zero and standard deviation of one which is limited to within three standard deviations of the mean). The prescribed errors are derived by averaging the errors in the various observing systems during FGGE; the temperature errors are from Bengtsson et al. (1982); the height, wind, and humidity errors were acquired from Baker et al. (1987).

TABLE 2. Rms error estimates as a function of height. The wind (u, v) height (z), and moisture (q) errors are derived by averaging the errors of different observing systems given by Baker et al. 1987 (Table 5). The temperature (T) errors are derived in a similar fashion from Bengtsson et al. 1982 (Table 1).

Pressure (mb)	u, v (m s^{-1})	T (C)	z (m)	q (g kg^{-1})
50	5.0	2.8	79.8	—
70	5.0	2.5	84.3	—
100	5.0	2.0	66.1	—
150	5.0	1.9	57.0	—
200	5.0	1.9	53.7	—
250	5.0	1.9	51.6	0.1
300	5.0	1.8	47.8	0.2
400	4.9	1.8	39.8	0.3
500	3.8	1.8	32.1	0.9
700	3.3	1.7	22.1	1.3
850	3.1	1.8	15.8	1.7
1000	2.8	2.3	8.0	1.7

The impact of random errors is determined by taking the difference between the budget results with random errors added and the original (baseline) results. The rms errors in S_A and $\mathrm{div}F_A$ during SOP I are negligible—less than 1 and 3 W m^{-2}, respectively, in all seven budget regions. Hastenrath (1980) estimated the rms error in the annual atmospheric energy flux divergence to be 5 W m^{-2} in a belt extending from 0°–30°N. Our smaller estimate may result from neglecting the dependence of the total rms error on time, latitude, longitude and the GLA data assimilation procedure.

A systematic error introduced at all grid points propagates through the budget calculations, causing the same bias in the value of $\mathrm{div}F_A$. Systematic errors that vary with location or height may have a more complex and severe effect on the budget computations. The largest errors in $\mathrm{div}F_A$ are likely to be due to systematic errors in the wind field (Lorenc and Swinbank 1984); we will focus on one well-documented bias in wind velocity estimates.

Kållberg et al. (1982), Halem et al. (1982), and other investigators have found that during the FGGE year, satellite cloud track motions generally underestimated the wind speed, especially in the vicinity of jet streams. Two possible explanations for this bias are the incorrect assignment of cloud height and that cirrus cloud motions may be slower than the actual wind. Satellite cloud motions are the primary source of wind data over the oceans but are of limited importance over continents (e.g., cloud tracked winds are not included in the GLA analysis over North America and northern Asia). A rigorous analysis of cloud track wind bias is beyond the scope of this paper. Instead, a simple approach is taken to examine the sensitivity of the budget results to systematic wind errors; i.e., wind

speeds from the 6-hour forecast are reduced by 10% at all grid points over the oceans and ice sheets but are left unchanged over land.

The systematic "error" in $\text{div}F_A$ is computed for SOP I by subtracting the original energy divergence from the divergence computed with reduced wind speeds over the oceans. The altered wind speeds caused very large errors, on the order of several hundred W m^{-2}, in the uncorrected sensible and geopotential energy flux divergence estimates. The mass balance correction significantly reduced but did not eliminate these errors. The mass corrected values for the individual energies and the total flux divergence during SOP I are shown in Table 3. The errors in the kinetic and latent energy divergence are small, generally less than 2 and 5 W m^{-2}, respectively. The errors in sensible and geopotential energy divergence exceeded 10 W m^{-2} in several regions, but are always of opposite sign and thus partially cancel. The systematic error in $\text{div}F_A$ exceed 10 W m^{-2} over North America and the North Pacific (and was greater than 20 W m^{-2} in additional budget regions located over the Pacific north of 30°N, the Greenland Sea and Europe), regions with relatively high wind speeds. This experiment indicates that systematic errors in the wind field can have a significant impact on the atmospheric energy divergence.

Wyrtki and Uhrich (1982) assessed the uncertainty of ocean heat storage estimates by evaluating measurement and sampling errors and by comparing simultaneous observations. They found that both instrument error and environmental variability on small time and space scales have a large impact on the computation of ocean heat storage. Wyrtki and Uhrich estimated that the maximum error in the monthly mean values of S_O is on the order of 100 W m^{-2} and concluded that it was not feasible to compute S_O on a monthly basis but that such estimates were possible over a complete heating or cooling season (6 months).

TABLE 3. The systematic "errors" in the individual and total energy flux divergence (W m^{-2}) for the budget regions during SOP I. The error values are obtained by subtracting the original energy flux divergence from the energy divergence when the grid point wind speeds are reduced by 10% over the oceans.

Region	Kinetic	Sensible	Potential	Latent	Total
North Atlantic	1	−9	13	−2	2
North America	−2	10	−25	−1	−18
North Pacific	3	−27	43	−6	13
Eurasia	−2	8	−17	2	−9
S. Atlantic	0	−8	11	−4	−1
S. Pacific	1	0	0	−1	−1
Indian Ocean	0	−3	3	−1	0
S. Africa	0	−1	0	0	0
S. America	0	5	−8	3	1
Australia	0	11	−16	4	−2
Antarctic Ocean	0	3	−5	1	1

2) MODEL ERRORS

The 6-hour GLA forecast provides estimates of variables in data poor regions but introduces errors inherent to numerical models. The finite-difference scheme and relatively coarse horizontal resolution are believed to adequately represent the general circulation over the brief duration of the forecast. However, the poor vertical resolution in the boundary layer may significantly degrade energy budget calculations.

Errors in the GLA GCM short-range forecasts have been quantified by Baker et al. (1987; Table 4). Rms error estimates in the 6-hour forecasts of geopotential height, wind and specific humidity were obtained for 30° latitude bands. The errors were derived by taking the difference between 6-hour forecasts and rawinsonde data over land for twelve periods during January 1979. The height errors range from approximately 10 m at 1000 mb to between 80 and 100 m at 50 mb. The errors in u and v are dependent on height and latitude and vary between 3 and 12 m s^{-1}. The largest wind and height errors are in the latitude band between 30°S and 60°S.

We investigated the impact of model errors on the atmospheric energy balance by taking the difference between the energy flux divergence computed from the analysis (when the data are first assimilated onto the model grid) with the divergence values obtained from the 6-hour forecast that verifies at that time. These differences ("errors") during SOP I are shown in Table 4. The large errors in the flux divergence of geopotential energy are mainly compensated by errors of opposite sign in the sensible heat flux divergence. The errors in these two terms exceed 40 W m^{-2} in several regions. The errors in the total divergence are much lower, less than 10 W m^{-2} with the exception of the North Pacific and South American regions. The large errors in the N. Pacific may result from differences between the analysis and the 6-hour forecast over the west coast of North America and the northeast Pacific (Halem et al. 1982).

Care must be taken in interpreting these results, because errors in the data analyses may obscure model errors. As pointed out by Halem et al. (1982), data which contain large land–sea contrasts in coverage may give rise to spurious waves in the initial conditions, which could then adversely affect the model forecast. In addition, small "model errors" occur in data poor regions, as the first-guess field and the analysis are nearly identical.

Another important source of model error results from the parameterization of diabatic processes, including radiation, cloud formation, and the surface sensible and latent heat flux. The accuracy of the GLA GCM estimates of shortwave radiation absorbed by the earth–atmosphere system (SW), outgoing longwave radiation (LW_T) and net radiation at the top of the

TABLE 4. The model errors in the individual and total energy flux divergence (W m^{-2}) for the budget regions during SOP I. The error values are obtained by subtracting the energy flux divergence computed from the 6-hour forecast (first guess) from the energy divergence obtained from the verifying analysis.

Region	Kinetic	Sensible	Potential	Latent	Total
North Atlantic	−1	5	0	−4	0
North America	0	23	−28	11	7
North Pacific	−1	17	−41	−1	−26
Eurasia	1	8	−12	0	−3
S. Atlantic	0	13	−15	4	2
S. Pacific	0	−6	10	1	5
Indian Ocean	0	−48	70	−12	10
S. Africa	0	−12	12	−4	−4
S. America	0	−73	110	−18	18
Australia	0	40	−60	10	−9
Antarctic Ocean	0	16	−26	8	−1

atmosphere (F_T) are assessed by comparing them with concurrent satellite measurements. The satellite data were collected by the Earth Radiation Budget (ERB) instrument package on board the sun-synchronous Nimbus 7 satellite. Observations were made simultaneously by two separate instrument packages, the fixed wide field of view (WFOV) and scanning narrow field of view (NFOV) radiometers. The raw data were processed to calculate radiation values for 2070 equal area sections, each approximately 500 km^2, which cover the entire globe. The ERB experiment, including instrument characteristics, data processing, and data quality is discussed in Arking and Vermury (1984), Jacobowitz et al. (1984a), Jackobowitz et al. (1984b), and Kyle et al. (1985).

The WFOV, NFOV, and GLA GCM estimates of the shortwave, longwave, and net radiation are presented in Fig. 5 for the North Atlantic, North America, North Pacific, and Eurasian regions during SOP I and II. The NFOV and WFOV estimates are in relatively good agreement, though some systematic differences between the two are evident. The WFOV regional estimates of SW during SOP I and SOP II average approximately 10 W m^{-2} higher than the NFOV SW values, and the WVOF LW_T exceed the NFOV LW_T values by an average of 3 W m^{-2}, leading to a disparity of 7 W m^{-2} in the F_T estimates between the two instruments. The differences in the NFOV and WFOV observations may be partially attributed to calibration errors, degradation of the WFOV channels, absorption of solar radiation which is subsequently reradiated onto the sensors, and reduced NFOV coverage during January through April. In addition, the WFOV instrument has an actual resolution that is wider than 4.5° and thus detects radiant energy from outside the budget region.

The net radiation estimates obtained from the GLA GCM are generally much greater than the ERB measurements (Fig. 5); the GLA bias averages over 25 (35) W m^{-2} when compared with the WFOV (NFOV) measurements for all seven budget regions during SOP I and SOP II. The majority of the GLA-WFOV bias, 22 W m^{-2}, results from excessive absorption of SW, while the LW_T biases are much smaller, with values of +3 W m^{-2} during SOP I and −7 W m^{-2} during SOP II. The SW bias is reduced by approximately 5–15 W m^{-2} in the sigma coordinate analysis (see section 4.c.3) depending on the location and time of year. The SW values, available from the GLA pressure history tapes, were obtained by interpolating the absorbed shortwave radiation from sigma to pressure levels. By saving the layer absorption instead of the flux values at the pressure levels, information concerning the thickness of the absorption layers was lost. Integrating over the more numerous but narrower pressure layers in the upper atmosphere resulted in a greater total absorbed shortwave radiation in pressure than in sigma coordinates.

The SW biases are most pronounced during the summer over the oceans; the SW GCM exceed the ERB estimates by over 50 W m^{-2} in the North Atlantic and North Pacific regions during SOP II. Weare (1988) found that the University of California at Los Angeles (UCLA) GCM also overestimated F_T and SW when compared with satellite data, especially at high latitudes over the oceans. He linked these discrepancies to the model's underestimation of the total cloudiness and the parameterization of the radiation effects of clouds. Underestimating cloud amounts has the greatest impact on SW during the summer because there is more solar radiation to reflect to space, and over the oceans because the difference in albedo between clouds and the underlying surface is greater over water than land.

Weare (1988) found that the UCLA GCM values of shortwave radiation absorbed by the ocean exceeded surface marine reports by 20 W m^{-2} over most of the Pacific between 30°N and 40°S. Estimates of SW_S from the GLA assimilated datasets appear to have a large positive bias when they are visually compared with the atlas of Esbensen and Kushnir (1981). The overestimation of shortwave radiation absorbed by the ocean propagates through the budget calculations, causing systematic errors in the estimates of the flux divergence and transport of heat by the ocean.

3) UNCERTAINTIES IN THE BUDGET METHOD

Inaccuracy is introduced into the energy balance estimates by the assumptions and numerical approximations used in the column budget method. The energy balance components may also be sensitive to the size and location of the budget column.

The large spatial variability of some of the atmospheric terms, especially $\mathrm{div}F_A$ (see Oort 1983, Fig. 17b; or Burridge 1985, Fig. 5), makes the energy balance calculations sensitive to the location of the budget

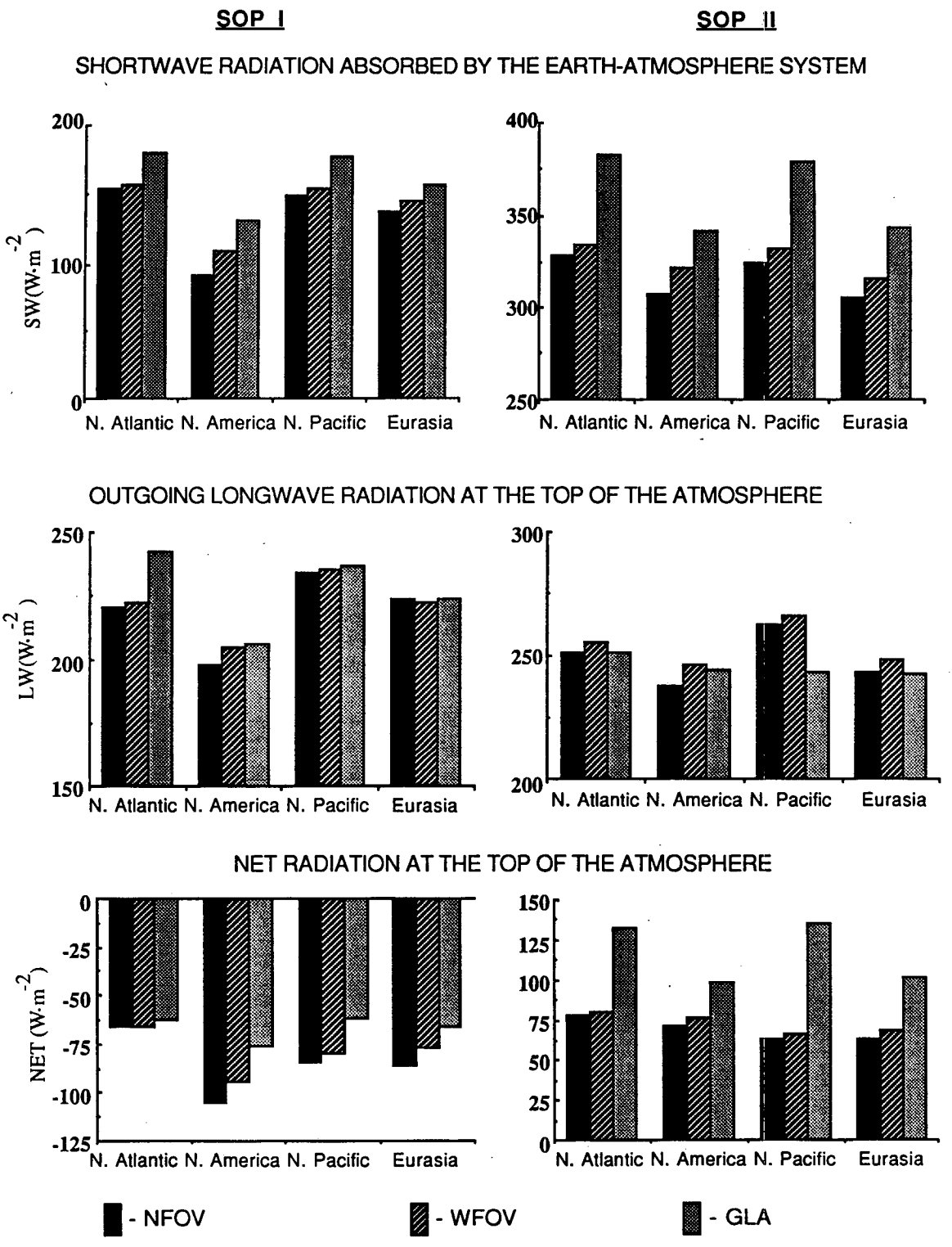

FIG. 5. Shortwave, longwave, and net radiation (W m^{-2}) computed from the WFOV and NFOV instruments, part of the Earth Radiation Budget (ERB) experiment, and from the GLA GCM during SOP I and SOP II.

column. Bretherton et al. (1982) estimated that small changes in the regional boundaries could alter divF_A by as much as 25 W m^{-2}. In our analysis, several closely located regions in the North Pacific (not presented) had divF_A values which differed by 10 to 15 W m^{-2} during both SOP I and II.

Differences between the numerical methods used to obtain the energy budget components and those employed by the GLA GCM may cause inconsistencies in the budget results, as the mass and energy conservation requirements in the model no longer apply. The differences between the energy budget and GLA GCM calculations, summarized in Table 5, include the data levels (σ vs p), method and limits of vertical integration, and the finite-differencing approximation. The impact of these differences on the budget results are examined by recomputing the energy balance on the models' sigma levels using the same vertical integration and fourth-order differencing scheme that is employed by the GLA GCM.

The vertical profiles of the (uncorrected) mass-weighted total energy flux divergence in pressure and sigma coordinates during July, 1979 are shown in Fig. 6. Divergence profiles are presented for the North Atlantic, North America, North Pacific, and Eurasian sectors. The results show fairly similar profiles over the oceanic regions but are considerably different over the land areas, especially North America. It appears that mountainous regions are especially sensitive to the numerical procedures, particularly the σ to p interpolation. The profiles indicate energy flux divergence in the lower troposphere (positive values) and convergence over most of the troposphere over the oceanic regions, with the reverse pattern over Eurasia. However, the North American profile indicates energy divergence (convergence) in the lower (upper) troposphere opposite to the expected energy transport over continents in summer.

A comparison of the July values of the (mass corrected) flux divergence of sensible, geopotential, latent, and total energy in σ and p coordinates is made in Table 6. Before the correction was applied the energy divergence values were very different in the two coordinate systems (>100 W m^{-2} in several regions). With the correction, the difference between σ and p coordinate estimates of the individual and total energy divergence are generally less than 20 W m^{-2}.

TABLE 5. The differences between the GLA GCM and the energy budget analysis in pressure coordinates.

Characteristic	GLA GCM	Energy budget
–data levels	9 sigma level	12 pressure levels (interpolated from σ levels)
–integration:		
method	midpoint rule	cubic spline
upper limit	10 mb	50 mb
lower limit	surface pressure minus 10 mb	average surface pressure
–finite differencing	fourth order	second order

In the last three columns of Table 6 the July values of sensible heat (SH) + latent heat (LH) obtained as residuals from the atmospheric energy budget are compared with those obtained directly from the GLA GCM parameterizations. The budget estimates of $SH + LH$ are derived from Eqs. (2.2) and (2.9) where the net surface radiation values, R in Eq. (2.9), are provided by the model. Surprisingly, the sigma values show no improvement over those obtained from the pressure analysis, as the $SH + LH$ estimates from both analyses differ considerably (rms differences of 30–35 W m^{-2} for the seven budget regions) from the GCM results. The surface flux estimates from the σ budget analysis and from the model should be identical in principal; the diabatic sources in the GCM, including the surface energy flux, are balanced by the storage and flux divergence of energy. This balance holds at all forecast periods (recall that our calculations are performed with the 6-hour forecast) but not at the time of data insertion. The source of the differences between the residual and GCM fluxes is deemed to be the inconsistent manner in which the diabatic (e.g., SH, LH and SW) and dynamic quantities (e.g., T, q, $\mathbf{V}$, gz) are stored on the GCM history tapes. The mass balance correction, S_A, and divF_A in the budget equations are computed from instantaneous dynamic quantities which are saved at 6-hour intervals, while the diabatic terms are stored as averages over the previous six hours. In addition, the Shapiro and polar filtering operations are not properly included as additional source/sink terms in the budget equations.

5. Summary and conclusion

The energy balance of the earth–atmosphere system during SOP I (1/5/79–3/5/79) and SOP II (5/1/79–7/31/79) was examined for selected regions around the globe. The column budget technique described by Oort and Vonder Haar (1976) provided estimates of the time tendency and flux divergence of energy in the atmosphere and ocean, and the air–sea energy flux. The atmospheric budget terms were computed from the GLA level IIIb analysis using the first-guess (6-hour forecast) fields. The ocean heat storage was calculated from a long-term record of oceanographic temperature observations. The air–sea flux and the oceanic energy flux divergence were computed as residuals. Sensitivity tests, error analyses, and comparisons with observations and other budget studies were employed to examine the accuracy and physical consistency of the energy balance terms.

The budget components provide information about the seasonal energy exchange between continental and

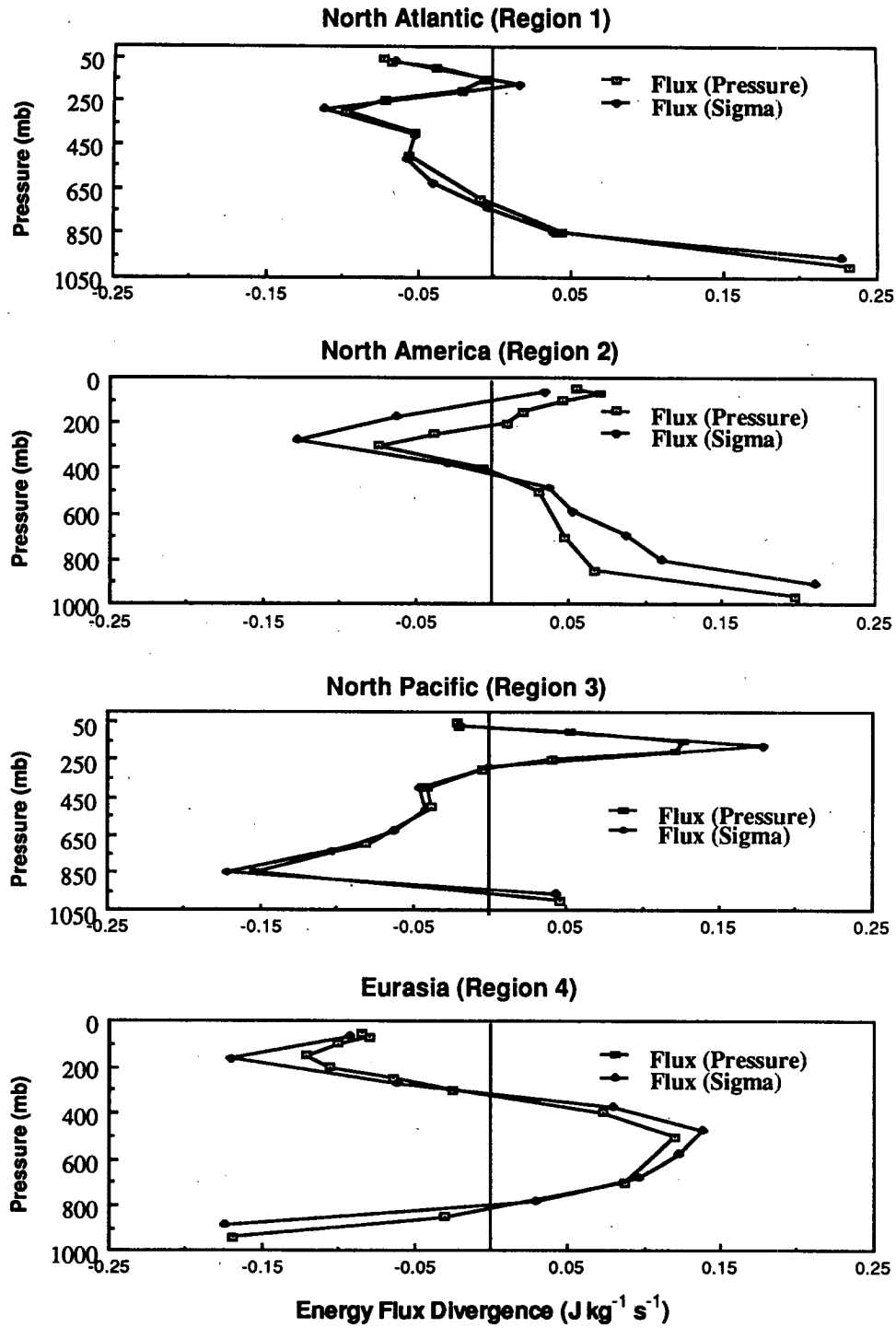

FIG. 6. The uncorrected total energy flux divergence profile (J kg^{-1} s^{-1}) for July 1979 for regions 1–4.

oceanic regions. In the Northern Hemisphere during winter, large quantities of energy (>100 W m^{-2}) in the midlatitude oceans are transferred to the overlying atmosphere. The atmosphere then transports the energy to the continental heat sinks. In summer, energy imparted from the warm continents to the overlying air is exported to the cooler oceanic regions. The seasonal exchange of energy between continents and

TABLE 6. The flux divergence of sensible, geopotential, latent, and total energy in pressure (p) and sigma (σ) coordinates. Also shown are the surface sensible plus latent heat flux ($SH + LH$) computed as residuals from the p and σ coordinate energy budgets using Eqs. (2.2) and (2.9) and from bulk aerodynamic formulae utilized by the GLA GCM. The results are for July 1979 with units of W m^{-2}.

	Energy flux divergence										
	Sensible		Potential		Latent		Total		($SH + LH$)		
Region	p	σ	p	σ	p	σ	p	σ	p	σ	GCM
North Atlantic	35	50	−68	−99	10	20	−22	−29	101	100	84
North America	57	66	−31	−55	10	21	45	32	148	153	157
North Pacific	−83	−73	75	61	20	−26	−41	−39	77	94	64
Eurasia	76	74	−52	−49	−33	−9	33	15	125	129	157
SH Ocean	174	162	−238	−219	69	70	5	13	143	160	119
SH Land	124	141	−170	−193	29	24	−13	−25	107	103	130
Antarctic Ocean	−34	−31	45	30	−20	−23	−11	−25	131	123	65

oceans appeared to be present but substantially weaker in the Southern Hemisphere due to the limited land mass and, therefore, smaller air–sea contrasts.

The effects of the mass balance correction and the individual energy flux terms on the total flux divergence were examined and then compared with other analyses. *A correction applied to conserve mass in the atmospheric column proved essential to obtaining reasonable energy flux divergence estimates.* The sensible and geopotential energy flux divergence generally had large magnitudes but opposite signs, tending to balance each other. Over North America and the North Pacific the corrected flux divergence of sensible and geopotential energy were markedly different from the values obtained from Met Office and ECMWF analyses (Lorenc and Swinbank 1984), though the total flux divergence values differed by less than 20 W m^{-2} for the four Northern Hemisphere regions.

Deficiencies in the data and data assimilation procedure, the GLA GCM, and the column budget method were discussed and several experiments were performed to quantify the impact of these error sources on the energy balance results. Major sources of data error include instrument bias, such as the underestimation of the strength of the jet stream by cloud tracked winds and the poor vertical resolution of temperature soundings obtained from satellite sensors. Errors are introduced during the assimilation cycle by the interpolation of observations from pressure to sigma levels, excitation of spurious gravity oscillations, and model bias. Multiple observing systems with different data densities, observing frequencies and error characteristics further complicate the data assimilation process.

The results of an error analysis showed that random errors in the atmospheric variables mainly affected the wind divergence and were compensated by the mass balance correction. After applying the mass balance correction, the errors had a negligible impact (<3 W m^{-2} over a 2 month period) on the atmospheric energy flux divergence. In contrast, an analysis of systematic errors showed that a 10% decrease in the wind speeds over the oceans (a rough approximation of the negative bias introduced by cloud track winds) altered the energy flux divergence by more than 13 W m^{-2} in several regions.

The GLA model, while providing information in data poor regions, adds additional uncertainty to the budget calculations. Comparing the energy divergence estimates from the analysis and the 6-hour forecast indicated that model errors could significantly impact the geopotential and sensible energy flux divergence. The errors in these two terms mainly cancelled resulting in errors in the total flux divergence that were generally less than 10 W m^{-2} but exceeded 15 W m^{-2} in the North Pacific and South American regions. A major source of model error is the inaccurate representation of diabatic processes, especially cloud formation, precipitation, and radiation. The accuracy of the GLA GCM estimates of shortwave, longwave and net radiation were assessed by comparing them with concurrent satellite measurements from the ERB instrument package. The GLA estimates of net radiation exceeded the observed values by an average of 25 W m^{-2} in the seven budget regions, mainly resulting from excessive absorption of shortwave radiation. The shortwave biases were most pronounced during summer over the oceans, exceeding 50 W m^{-2} over the North Atlantic and Pacific. The bias in the radiation fields in the GLA model and other GCMs is likely linked to the parameterization of the optical properties and fractional coverage of clouds.

The procedures inherent to the column budget method are a potentially large source of uncertainty in the energy balance estimates. The flux divergence and storage of energy, computed from the difference between large numbers, are susceptible to error and sensitive to the size of the budget column. Small displacements in regional boundaries altered the total energy flux divergence by 5 to 15 W m^{-2}. The influence of the finite-difference approximations and vertical interpolation were examined by comparing the budgets in sigma coordinates using the GLA fourth-order finite

differencing and pressure coordinates using second-order differencing. The difference in the divergence estimates between the two analyses were generally less than 20 W m^{-2}.

The budget method was tested further by comparing the combined surface sensible and latent heat flux derived as residuals from the energy budget in sigma and pressure coordinates with those obtained directly from the model. The sigma values were thought to be more consistent with the model, as the same numerical methods and conservation principals were used in both. However, the estimates from the sigma and pressure budgets both differed from the GCM estimates by a rms value of approximately 30 W m^{-2}. This difference is believed to result from the coarse sampling frequency of the model history tapes and the inconsistencies in the way in which the dynamic and diabatic quantities were saved. Such errors can be reduced by calculating the budget quantities on-line and at each time step as the model integration precedes.

The error in the GLA GCM regional values of the net radiation at the top of the atmosphere is estimated to be between 20–50 W m^{-2}, depending on the season and location of the region. Estimates from satellites are more reliable. The difference between the two sensors aboard the ERB satellite averaged 7 W m^{-2} for the seven budget regions, in agreement with Oort and Vonder Haar (1976) and Ellis et al. (1978) who estimated the uncertainty in net radiation to be 10 W m^{-2}. Errors in the energy storage are believed to be small, generally less than 5 W m^{-2}. The atmospheric flux divergence of energy is an extremely difficult term to calculate, as systematic errors in the wind field can lead to large mass imbalances. Through our sensitivity studies and comparison with other analyses we estimate the error in energy divergence to be 15 to 25 W m^{-2}. Error propagation in the budget calculations leads to an uncertainty in surface energy flux between 20–40 W m^{-2}. An estimate of 30 W m^{-2} was obtained from the error evaluation of Hastenrath (1980). Bretherton et al. (1982) indicated that an error of 10 W m^{-2} or less in the ocean energy flux divergence was necessary to calculate the meridional heat transport to within a desired accuracy of 20%. It is not possible to obtain this degree of accuracy using the column budget method with current data sources, a conclusion also reached by Boer (1986) and Holopainen and Fortelius (1986).

Progress towards reducing the uncertainty in energy diagnostics and other climatic variables are closely associated with improvements in data assimilation methods and model parameterizations of physical processes. For example, optimum interpolation may help to identify and remove systematic errors in the data, while improved initialization procedures may be able to remove mass imbalances while maintaining the correct divergence structure.

Acknowledgments. We wish to thank Gerald Herman for his support, and John Kutzbach, Elizabeth Ebert, and R. Bradley Pierce for their comments and suggestions. The advice and computer expertise provided by the staff of the Goddard Laboratory for Atmospheres, including Lawrence Tackas, Jim Pfaetner and Menina Almeida is greatly appreciated.

The ERB satellite data were provided by Carolyn Ng, the Request Coordinator at the National Space Sciences Data Center. The calculations in this study were performed on the Amdahl-V6 computer at the Goddard Laboratory for Atmospheres, which is sponsored by the National Aeronautics and Space Administration. This research was conducted under NASA Grant NSG-5223, with additional support from NSF Grant ATM-86-03295.

REFERENCES

Alestalo, M., 1981: The energy budget of the earth–atmosphere system in Europe. *Tellus,* **33,** 360–371.

Arking, A., and S. K. Vermury, 1984: The Nimbus-7 ERB data set: A critical analysis. *J. Geophys. Res.,* **89,** 5089–5097.

Baker, W. E., 1983: Objective analysis and assimilation of observational data from FGGE. *Mon. Wea. Rev.,* **111,** 328–342.

——, S. C. Bloom, J. S. Woollen, M. S. Nestler, E. Brin, T. W. Schlatter and G. W. Branstator, 1987: Experiments with a three-dimensional statistical objective analysis scheme using FGGE data. *Mon. Wea. Rev.,* **115,** 272–296.

Bengtsson, L., M. Kanamitsu, P. Kallberg and S. Uppala, 1982: FGGE 4-dimensional data assimilation at ECMWF. *Bull. Amer. Meteor. Soc.,* **63,** 29–43.

Boer, G. J., 1986: A comparison of mass and energy budgets from two FGGE data sets and a GCM. *Mon. Wea. Rev.,* **114,** 885–902.

Bretherton, F. P., D. M. Burridge, J. Crease, F. W. Dobson, E. B. Kraus and T. H. Vonder Haar, 1982: The "CAGE" experiment: a feasibility study. World Climate Program, WCP-22, WMO, Geneva, 95 pp.

Bryan, K., 1962: Measurements of meridional heat transport by ocean currents. *J. Geophys. Res.,* **67,** 3403–3414.

Burridge, D. M., 1985: Energy flux divergence calculations from ECMWF analyses for the FGGE year. WMO Global Weather Experiment Scientific Seminar, Helsinki. Garp Special Report No. 42, WMO, Geneva; pp. II 1–14.

Carissimo, B. C., A. H. Oort and T. H. Vonder Haar, 1985: Estimating the meridional energy transport in the atmosphere and oceans. *J. Phys. Oceanogr.,* **15,** 82–91.

Cressman, G. P., 1959: An operational objective analysis scheme. *Mon. Wea. Rev.,* **87,** 329–340.

Ellis, J. S., T. H. Vonder Haar, S. Levitus and A. H. Oort, 1978: The annual variation in the global heat balance of the earth. *J. Geophys. Res.,* **83,** 1958–1963.

Esbensen, S. K., and Y. Kushnir, 1981: The heat budget of the global ocean: an atlas based on estimates from surface marine observations. Report No. 29, Climatic Research Institute, Oregon State University, Corvalis, 219 pp.

Gruber, A., 1970: The energy budget over the Florida Peninsula when a convective regime dominates. *J. Appl. Meteor.,* **9,** 401–416.

Halem, M., E. Kalnay, W. E. Baker and R. Atlas, 1982: An assessment of the FGGE satellite observing system during SOP-1. *Bull. Amer. Meter. Soc.,* **63,** 407–426.

Hastenrath, S. L., 1966: On general circulation and energy budget in the area of the Central American seas. *J. Atmos. Sci.,* **23,** 694–711.

——, 1980: Heat budget of tropical ocean and atmosphere. *J. Phys. Oceanogr.*, **10,** 159–170.

——, 1982: On the meridional heat transport in the world ocean. *J. Phys. Oceanogr.*, **12,** 922–927.

Hollingsworth, A., A. C. Lorenc, M. S. Tracton, K. Arpe, G. Kats, S. Uppala and P. Kållberg, 1985a: The response of numerical prediction systems to FGGE level IIb data. Part 1: Analyses. *Quart. J. Roy. Met. Soc.*, **111,** 1–66.

Holopanien, E., and C. Fortelius, 1986: Accuracy of estimates of atmospheric large-scale energy flux divergence. *Mon. Wea. Rev.*, **114,** 1910–1921.

Hsuing, J., 1985: Estimates of global oceanic meridional heat transport. *J. Phys. Oceanogr.*, **15,** 1405–1413.

Jacobowitz, H., V. Soule, H. L. Kyle, F. B. House and the Nimbus-7 ERB Experiment Team, 1984a: The Earth Radiation Budget (ERB) Experiment: An overview. *J. Geophys. Res.*, **89,** 5021–5038.

——, R. J. Tighe and the Nimbus-7 Experiment Team, 1984b: The earth radiation budget derived from the Nimbus-7 experiment. *J. Geophys. Res.*, **89,** 4997–5010.

Japanese Meteorological Agency, 1981: Results of an impact study on analysis and prediction of various combinations of the observing systems. *International Conference of Preliminary FGGE Data Analysis and Results,* Bergen, Norway, 23–27 June, 1980. WMO, Geneva, pp. 88–104.

Kållberg, P., S. Uppala, N. Gustafsson and J. Pailleux, 1982: The impact of cloud tracked wind data on global analyses and medium range forecasts. ECMWF Tech. Rept. 34, Reading, England. 60 pp.

Kalnay, E., R. Balgovind, W. Chao, D. Edelmann, J. Pfaendtner, L. Takacs and K. Takano, 1983: Documentation of the GLAS fourth order general circulation model. NASA Tech. Memo. 86064, NASA/Goddard Space Flight Center, Greenbelt, MD, 359 pp.

Kyle, H. L., P. E. Ardanuy and E. J. Hurley, 1985: The status of the Nimbus-7 Earth-Radiation-Budget data set. *Bull. Amer. Met Soc.*, **66,** 1378–1388.

Lau, N-C., and A. H. Oort, 1981: A comparative study of observed Northern Hemisphere circulation statistics based on GFDL and NMC analyses. Part 1: the time mean fields. *Mon. Wea. Rev.*, **109,** 1380–1403.

Levitus, S., 1982: *Climatological Atlas of the World Ocean.* NOAA Prof. Paper No. 13, U.S. Government Printing Office, Washington, D.C., 173 pp.

Lorenc, A. C., and R. Swinbank, 1984: On the accuracy of general circulation statistics calculated from FGGE data—a comparison of results from two sets of analyses. *Quart. J. Roy Met. Soc.*, **110,** 915–942.

Lyne, W. H., R. Swinbank and N. T. Birch, 1982: A data assimilation experiment and the global circulation during the FGGE special observing periods. *Quart. J. R. Met. Soc.*, **108,** 575–594.

Newell, R. E., J. W. Kidson, D. G. Vincent and G. J. Boer, 1974: *The general circulation of the tropical atmosphere and interactions with the extratropical latitudes,* Vol. 2. The MIT Press, Cambridge Mass., 371 pp.

O'Brien, J., 1970: Alternative solutions to the classical vertical velocity problem. *J. Appl. Meteorol.*, **9,** 197–203.

Oort, A. H., 1978: Adequacy of the rawinsonde network for global circulation studies tested through numerical model output. *Mon. Wea. Rev.*, **106,** 174–195.

——, 1983: *Global Atmospheric Circulation Statistics, 1958–1973.* NOAA Professional Paper 14, U.S. Government Printing Office, Washington, D.C., 180 pp.

——, and T. H. Vonder Haar, 1976: On the observed annual cycle in the ocean–atmosphere heat balance over the Northern Hemisphere. *J. Phys. Oceanogr.*, **6,** 781–800.

Palmén, E., and C. W. Newton, 1969: *Atmospheric circulation systems.* Academic Press, 603 pp.

Phillips, N. A., L. M. Mc Millin, A. Gruber and D. Q. Wark, 1979: An evaluation of early operational temperature soundings. *Bull. Amer. Meteor. Soc.*, **60,** 1188–1197.

Sävijarvi, H., 1982: The mass balance in diagnostic studies: An example of analysed and forecast data calculations. *Tellus,* **34,** 540–544.

——, 1983: The atmospheric energy budgets over North America, the North Atlantic and Europe based on ECMWF analyses and forecasts. *Tellus,* **35,** 29–50.

Schlatter, T. W., 1981: An assessment of operational TIROS-N temperature retrievals over the United States, *Mon. Wea. Rev.*, **109,** 110–119.

Sellers, W. D., 1965: *Physical Climatology,* The University of Chicago Press., 272 pp.

Shapiro, R., 1970: Smoothing, filtering and boundary effects. *Rev. Geophys. and Space Phys.*, **8,** 359–387.

Vonder Haar, T. H., and A. H. Oort, 1973: New estimates of annual poleward energy transport by Northern Hemisphere Oceans. *J. Phys. Oceanogr.*, **2,** 169–172.

Weare, B. C., 1988: A comparison of radiation variables calculated in the UCLA General Circulation Model to observations, *J. Climate,* **1,** 485–499.

White, R. M., and B. Saltzman, 1956: On conversions between potential and kinetic energy in the atmosphere. *Tellus,* **8,** 357–363.

Wyrtki, K., and L. Uhrich, 1982: On the accuracy of heat storage computations. *J. Phys. Oceanogr.*, **12,** 1411–1416.